Electronic Journal of Differential Equations, Vol. 2023 (2023), No. 15, pp. 1–24.
ISSN: 1072-6691. URL: https://ejde.math.txstate.edu or https://ejde.math.unt.edu

ESTIMATION OF PLATE PARAMETERS FROM VERTICAL DISPLACEMENT DATA USING A FAMILY OF PLATE MODELS

LUTHER WHITE, TETYANA MALYSHEVA, LEIF KARLSTROM

Abstract. We develop a method for estimation of parameters of an elastic plate resting on a Winkler-type elastic foundation solely from data on the vertical displacements of the plate. The method allows one to estimate components of the external body force density field, plate thickness, elastic foundation stiffness parameters, horizontal displacements of the plate, and stresses. The key idea of the method is that multiple plate models are used simultaneously, namely the proposed reduced three-dimensional (R3D) plate model, the Mindlin plate model, and the thin plate model. The three plate models form a hierarchy of elastic plate models based on assumptions imposed on stresses, with the R3D plate model being the most generalized model and the thin plate model being the most constrained one. The hierarchical relationship among the plate models allows one to incorporate prior information into the estimation technique. The applicability of the proposed estimation method is illustrated by a numerical example.

1. Introduction

We consider a three-dimensional elastic plate of non-uniform thickness resting on an elastic foundation and subjected to an external force. Our objective is to estimate the components of the external body force field, plate thickness, and the stiffness parameters of the foundation solely based on the measurements of the vertical displacement of the plate. The original motivation for our work arises from geophysics applications dealing with modeling and analysis of sill and laccolith deformation, where models of an elastic plate lying on an elastic foundation are used to capture the deflection of rock strata above a magma-filled intrusion in the subsurface [5, 12, 23]. In these applications, the goal is generally to infer the geometry of the intrusion, the force distribution generating deformation, and the material parameters of the surrounding rock, often solely from data on the earth surface. Magmatic intrusions exhibit a wide variety of shapes and depths, and often occur repeatedly over prolonged volcanic episodes. Plate models are an attractive framework to capture both isolated intrusions and sequences [24].

In fact, the problems of estimation of external forces and parameters for plate models have been of great practical interest in all fields of science and engineering where elastic plate models are employed. The identification of impact forces acting

2020 *Mathematics Subject Classification.* 35Q74, 74B05, 74K20, 35Q86, 86-10.
Key words and phrases. Elastic plate model; linear elasticity; parameter estimation; force estimation; laccolith.

Submitted February 28, 2022. Published February 17, 2023.

on elastic plate structures - an important problem in impact engineering and structural health monitoring - was studied in [11, 16, 20, 37, 38]. In [20], the iterative inversion method of deconvolution with Green's functions of the medium was presented to determine oblique force acting on a surface of an infinite plate. In [16], the impact load on a thick plate was determined inversely using theoretical Green's function and simulated wave form under the assumption that the direction of the force is the only vertical. In [37], two methods - theoretical using Green's functions and experimental - were developed to determine the impact-force history for thin plates based on the strain response. In [38] the transverse impact force history was determined for a rectangular Reissner-Mindlin plate based on the strain response using the eigenmode expansion method. In [11], the loading source of an infinite beam on an elastic foundation was inversely identified from given information of vertical deflection of the infinite beam using Tikhonov's regularization. The work [11] was motivated by offshore hydrodynamic applications dealing with very large floating structures and ice plates in waves.

Available literature on estimation of thickness of elastic plates is mostly limited to geoscience problems of estimation of the effective elastic thickness Te of Earth's lithosphere modeled by thin elastic plates [3, 32]. Evaluation of Te is of great importance in geophysics as it has profound influence on the deformation and coupling of adjacent blocks within the theory of plate tectonics [3]. Common methods for estimation of Te involve comparison of gravity anomalies and topography associated with vertical deflection of thin elastic plates [32].

To describe the plate-base interaction, we utilize a Winkler-type foundation model represented by a spring layer attached to the bottom of the plate and to the top of the rigid base. The Winkler foundation models are widely used in different fields of engineering to analyze beams, plates, and slabs resting on a soil medium [1, 28, 39]. The Winkler elastic foundations are also commonly employed in geophysics in modeling of laccolith and sill formations to describe weak sedimentary layers along which laccolith or sill is emplaced [5, 12]. The behavior of the Winkler foundation is characterized by the spring constant called the subgrade modulus or the foundation stiffness parameter. Many researchers have made great efforts to evaluate the subgrade modulus [2, 5, 25, 31, 36, and the references therein]. The developed formulas are based on the elastic properties and geometry of the foundation.

To our best knowledge, the present paper is the first one that attempts to estimate the external force field acting on an elastic plate, plate thickness, and elastic foundation stiffness parameters solely based on the measurements of the vertical displacement of the plate. The main difficulty here comes from the fact that a single plate model does not suffice to solve any of the given estimation problems. To overcome this obstacle, we propose the estimation method in which multiple plate models are used in conjunction. Specifically, we employ the family of three plate models resting on a Winkler-type elastic foundation: the thin plate model, the Mindlin plate model, and the proposed reduced three dimensional (R3D) plate model.

The classical theory of elastic thin plates (see, for example, [13, 15]) assumes that comparatively small forces on plate surface are needed to bend it and therefore, transverse shear and normal stresses are negligible. The Mindlin plate theory [13, 21], also known as the first-order shear deformation theory, takes into account

transverse shear effects, but retains zero transverse normal stress assumption and requires a shear correction factor. Although the Mindlin plate model provides sufficiently accurate results for moderately thick plates, it is not convenient to use due to the difficulty of determining an accurate shear correction factor [33]. The proposed R3D plate model does not impose zero stress assumptions existing in the thin and Mindlin plate models and does not involve a shear correction factor. At the same time, the R3D plate model preserves displacement assumptions embedded into the Mindlin plate model, thereby maintaining the simplicity of the first-order shear deformation theory. A distinguishing feature of the plate models under consideration is that, instead of stresses, the body force densities are used to capture external forces acting on the plate. It is assumed that the body force density field has a functional form compatible with that of the plate displacement field.

The estimation method proposed in this paper involves the following steps. Initially, the three plate models are used to establish relations among normal displacements and normal and tangential force densities. For comparison of the three plate models, given normal vertical displacement data, we first estimate normal force densities from each of the three plate models under the explicit constraining assumption that tangential forces are zero. Next, the three weighted plate models are used jointly to estimate both normal and tangential force densities, where forces are not constrained. It is assumed, however, that the actual tangential components of the body force are independent of the actual model being applied. Under a further assumption that the differences between predicted normal body force densities from the different models should be small, estimations of implied plate thickness and the foundation stiffness parameters are carried out. In addition, as a byproduct of our estimation technique, estimates of the stresses and horizontal displacements of the plate are also derived.

Thus, the main contribution of this paper is the new and unique estimation method based on the simultaneous use of multiple elastic plate models, which allows one to estimate the components of an external force field acting on an elastic plate, plate thickness, elastic foundation stiffness parameters, as well as the stresses and horizontal displacements of the plate, solely from the measurements of the vertical displacement of the plate.

This article is organized as follows. In Section 2, we present the distributed parameter models for an elastic plate under consideration. The models are formulated in a variational form based on the principle of minimum total potential energy. The variational formulation allows one to consider more general situations, for example, with discontinuities, and provides a foundation for finite element approximations. In Section 3, the spatially discretized plate models are obtained by finite element approximations and represented by systems of algebraic equations. Ultimately, these are the models that are used in computations. In Section 4, we describe the techniques for estimation of model parameters from data on vertical displacement of the plate. In Section 5, we present a numerical example from the geoscience application to illustrate the applicability of the proposed method.

2. Plate model family

In this section we provide variational formulations of three distributed parameter elastic plate models: the R3D plate, the Mindlin plate, and the thin plate, resting on the Winkler-type foundation. The variational formulations are the basis for finite

element solutions and for our estimation of forces applied to an elastic medium from normal displacement data. The derivation of the R3D plate model is given in detail. Derivations of the Mindlin and thin plate models are well-known but are summarized to emphasize the differences.

We begin by fixing the following notation to be used throughout this paper. In what follows, boldface letters denote vectors, both variables and functions. In particular, $\mathbf{i}, \mathbf{j}, \mathbf{k} \in \mathbb{R}^3$ are reserved for the basic unit vectors in Cartesian coordinates with the z-axis pointing upwards. Subscripts x, y, and z represent partial derivatives, and superscript T means transpose. Let $\Omega_h = \Omega \times (-\frac{h}{2}, \frac{h}{2})$ be a bounded open cylindrical domain in $\mathbb{R}^3$ representing a homogeneous in a vertical direction and isotropic elastic plate of variable thickness h. We assume that region $\Omega \subset \mathbb{R}^2$ has a sufficiently smooth boundary $\partial\Omega$ and is large enough so that the plate undergoes negligible displacement on the boundary $\Gamma = \partial\Omega \times (-\frac{h}{2}, \frac{h}{2})$. We define the following spaces:

$$H = L^2(\Omega), \quad V_0 = H_0^1(\Omega), \quad \mathbf{H}_h = L^2(\Omega_h, \mathbb{R}^3), \quad \mathbf{V}_h = H^1(\Omega_h, \mathbb{R}^3)$$

with standard norms, and

$$\mathbf{V}_{h0} = \left\{ \mathbf{\Phi} \in \mathbf{V}_h : \mathbf{\Phi}|_\Gamma = 0 \right\}$$

with the norm $\|\cdot\|_{\mathbf{V}_{h0}}$ inherited from $\mathbf{V}_h$. The symbol $\|\cdot\|$ stands for the Euclidean norm.

Let the displacement at a point $(x, y, z) \in \Omega_h$ be expressed as a vector-valued function $\mathbf{u}$ given by

$$\mathbf{u}(x, y, z) = u(x, y, z)\mathbf{i} + v(x, y, z)\mathbf{j} + w(x, y, z)\mathbf{k}\,. \tag{2.1}$$

The displacement gradients are assumed to be small [9] so that higher-order powers of the displacements and their derivatives are neglected. Let $\boldsymbol{\varepsilon} = [\varepsilon_{ij}]_{i,j=1}^3$ and $\boldsymbol{\tau} = [\tau_{ij}]_{i,j=1}^3$ denote the strain and stress tensors, respectively. With the above assumptions, the strain-displacement relations for an isotropic material are expressed as

$$\boldsymbol{\varepsilon} = \frac{1}{2}(\nabla\mathbf{u} + \nabla\mathbf{u}^T) \tag{2.2}$$

and the stress-strain relations for an isotropic medium are given by

$$\boldsymbol{\tau} = \frac{E}{1+\nu}\left[\boldsymbol{\varepsilon} + \frac{\nu}{1-2\nu}(tr\boldsymbol{\varepsilon})I\right], \tag{2.3}$$

where E is Young's modulus, ν is Poisson's ratio, $tr\boldsymbol{\varepsilon}$ is the trace of the tensor $\boldsymbol{\varepsilon}$, and I is the identity tensor [6, 9]. We assume that E and ν may be spatially dependent.

The elastic strain energy of the plate is defined to be

$$\mathcal{V}_E(\mathbf{u}) = \frac{1}{2}\int_{\Omega_h} \boldsymbol{\tau}(\mathbf{u}) : \boldsymbol{\varepsilon}(\mathbf{u})\,\mathrm{d}V\,.$$

We assume that the plate is subjected to an external body force whose density is represented by

$$\mathbf{F}(x, y, z) = F_u(x, y, x)\mathbf{i} + F_v(x, y, z)\mathbf{j} + F_w(x, y, z)\mathbf{k}\,.$$

Then the work done on the plate by the above force is

$$\mathcal{W}(\mathbf{u}) = \int_{\Omega_h} \mathbf{F}\cdot\mathbf{u}\,\mathrm{d}V\,. \tag{2.4}$$

A Winkler-type elastic foundation connecting the plate with a rigid foundation is characterized by positive functions $\kappa_u(x,y)$, $\kappa_v(x,y)$, and $\kappa_w(x,y)$. These functions may be thought as spring coefficients indicating the stiffness of support from the elastic foundation. The potential energy functional associated with the elastic foundation is given by

$$\mathcal{V}_F(\mathbf{u}) = \frac{1}{2}\int_\Omega \mathbf{u}(x,y,-h/2)^T K_F \mathbf{u}(x,y,-h/2)\,\mathrm{d}A\,, \tag{2.5}$$

where

$$K_F(x,y) = \begin{bmatrix} \kappa_u(x,y) & 0 & 0 \\ 0 & \kappa_v(x,y) & 0 \\ 0 & 0 & \kappa_w(x,y) \end{bmatrix}. \tag{2.6}$$

The total potential energy of the plate is then defined as

$$\Pi(\mathbf{u}) = \mathcal{V}_E(\mathbf{u}) + \mathcal{V}_F(\mathbf{u}) - \mathcal{W}(\mathbf{u})\,. \tag{2.7}$$

To proceed further, we wish to express the total potential energy $\Pi(\mathbf{u})$ in terms of functionals on $\mathbf{V}_h$. The following assumption will be used throughout this article.

Assumption 2.1. $E, \nu, \kappa_u, \kappa_v, \kappa_w, \in L^\infty(\Omega)$, and $\mathbf{F} \in \mathbf{H}_h$.

Define the symmetric, continuous [27], bilinear form on $\mathbf{V}_h$ by

$$\alpha_E(\mathbf{u}, \mathbf{\Phi}) = \int_{\Omega_h} \boldsymbol{\tau}(\mathbf{u}) : \boldsymbol{\varepsilon}(\mathbf{\Phi})\,\mathrm{d}V\,.$$

Then the elastic strain energy can be expressed as

$$\mathcal{V}_E(\mathbf{u}) = \frac{1}{2}\alpha_E(\mathbf{u},\mathbf{u})\,. \tag{2.8}$$

Let $\gamma_0^{\mathrm{int}} : \mathbf{V}_h \to H^{1/2}(\partial\Omega_h, \mathbb{R}^3)$ be a trace operator [27] defined by

$$\gamma_0^{\mathrm{int}}(\mathbf{u}) = \mathbf{u}\big|_{\partial\Omega_h}, \quad \mathbf{u} \in \mathbf{V}_h\,.$$

Let $\partial\Omega_b = \Omega \times \{-\frac{h}{2}\}$ denote a part of the boundary $\partial\Omega_h$ corresponding to the bottom of the plate, and $\big|_{\partial\Omega_b}$ be a restriction operator from $H^{1/2}(\partial\Omega_h, \mathbb{R}^3)$ to $H^{1/2}(\Omega_b, \mathbb{R}^3)$. Then $\alpha_F : \mathbf{V}_h \times \mathbf{V}_h \to \mathbb{R}$ given by

$$\alpha_F(\mathbf{u}, \mathbf{\Phi}) = \int_\Omega \big[\big(\gamma_0^{\mathrm{int}}(\mathbf{u})\big)\big|_{\partial\Omega_b}\big]^T K_F \big(\gamma_0^{\mathrm{int}}(\mathbf{\Phi})\big)\big|_{\partial\Omega_b}\,\mathrm{d}A \tag{2.9}$$

defines a symmetric, continuous, bilinear form on $\mathbf{V}_h$. From (2.5) and (2.9), we have

$$\mathcal{V}_F(\mathbf{u}) = \frac{1}{2}\alpha_F(\mathbf{u},\mathbf{u})\,. \tag{2.10}$$

Finally, for every $\mathbf{F} \in \mathbf{H}_h$, we define a continuous linear functional f on $\mathbf{V}_{h0}$ by the pairing $\mathbf{\Phi} \mapsto \langle f, \mathbf{\Phi}\rangle$, where

$$\langle f, \mathbf{\Phi}\rangle = \int_{\Omega_h} \mathbf{F}\cdot\mathbf{\Phi}\,\mathrm{d}V\,. \tag{2.11}$$

Applying (2.4), (2.8), (2.10), and (2.11) to (2.7) yields

$$\Pi(\mathbf{u}) = \frac{1}{2}\alpha_E(\mathbf{u},\mathbf{u}) + \frac{1}{2}\alpha_F(\mathbf{u},\mathbf{u}) - \langle f, \mathbf{u}\rangle\,. \tag{2.12}$$

Under assumption that the plate experiences negligible displacement on the boundary Γ, admissible displacements are $\mathbf{u} \in \mathbf{V}_{h0}$. According to the principle

of minimum total potential energy, the displacement $\mathbf{u}$ that the region Ω_h undergoes satisfies

$$D\Pi(\mathbf{u})\mathbf{\Phi} = 0, \quad \forall\ \mathbf{\Phi} \in \mathbf{V}_{h0}\,, \tag{2.13}$$

where

$$D\Pi(\mathbf{u})\mathbf{\Phi} = \frac{d}{d\delta}\Pi(\mathbf{u} + \delta\mathbf{\Phi})\Big|_{\delta=0}$$

is the first variation of Π at $\mathbf{u}$. Applying (2.13) to (2.12), we arrive to the following variational (weak) equation for an elastic plate resting on a Winkler-type foundation.

$$\alpha_E(\mathbf{u}, \mathbf{\Phi}) + \alpha_F(\mathbf{u}, \mathbf{\Phi}) = \langle f, \mathbf{\Phi}\rangle, \quad \forall\ \mathbf{\Phi} \in \mathbf{V}_{h0}\,. \tag{2.14}$$

Recall Korn's inequality [4, 13] that states that there exists a positive constant κ such that for any $\mathbf{u} \in \mathbf{V}_{h0}$

$$\alpha_E(\mathbf{u}, \mathbf{u}) \geq \kappa\|\mathbf{u}\|^2_{\mathbf{V}_h}\,. \tag{2.15}$$

With (2.15) and $\alpha_F(\mathbf{u}, \mathbf{u}) \geq 0$, the bilinear form $(\alpha_E + \alpha_F)$ on $\mathbf{V}_h$ is symmetric, continuous and $\mathbf{V}_{h0}$-coercive. The Lax-Milgram theorem [30] applied to (2.14) immediately yields the well-posedness of the variational problem (2.14) associated with an elastic plate on a Winkler-type foundation.

To obtain variational formulations of the R3D, Mindlin, and thin plate models, we specialize displacements (2.1) to various subspaces of displacement functions. Henceforth, for convenience, we set

$$a = \frac{E}{(1+\nu)(1-2\nu)}, \quad \hat{a} = \frac{E}{1-\nu^2}, \quad b = \frac{E}{2(1+\nu)} \tag{2.16}$$

and

$$I_1 = h, \quad I_2 = \frac{h^2}{4}, \quad I_3 = \frac{h^3}{12}\,.$$

For the R3D plate model, we consider the components of the displacement vector $\mathbf{u}$ given by

$$\begin{aligned} u(x, y, z) &= zu_1(x, y)\\ v(x, y, z) &= zv_1(x, y)\\ w(x, y, z) &= w_0(x, y) \end{aligned} \tag{2.17}$$

with $u_1, v_1, w_0 \in V_0$. Here w_0 is the displacement of the mid-surface of the plate in the z-direction, u_1 and v_1 are rotations of the normal to the mid-surface of the plate about the x-axis and the y-axis, respectively. Substituting (2.17) into (2.2) and (2.3) yields, respectively, the following strain-displacement and stress-displacement relations

$$\begin{aligned} \varepsilon_{11} &= zu_{1x}, \quad \varepsilon_{12} = \frac{z}{2}(u_{1y} + v_{1x}),\\ \varepsilon_{22} &= zv_{1y}, \quad \varepsilon_{13} = \frac{1}{2}(u_1 + w_{0x}),\\ \varepsilon_{33} &= 0, \qquad \varepsilon_{23} = \frac{1}{2}(v_1 + w_{0y}), \end{aligned} \tag{2.18}$$

and

$$\begin{aligned} \tau_{11} &= za[(1-\nu)u_{1x} + \nu v_{1y}], \quad \tau_{12} = zb(u_{1y} + v_{1x}),\\ \tau_{22} &= za[\nu u_{1x} + (1-\nu)v_{1y}], \quad \tau_{13} = b(u_1 + w_{0x}),\\ \tau_{33} &= z\nu a[u_{1x} + v_{1y}], \qquad\qquad \tau_{23} = b(v_1 + w_{0y})\,. \end{aligned} \tag{2.19}$$

For compatibility with the assumed displacements, we consider the external force densities in the form

$$\begin{aligned} F_u(x,y,z) &= zf_u(x,y) \\ F_v(x,y,z) &= zf_v(x,y) \\ F_w(x,y,z) &= f_w(x,y) \end{aligned} \tag{2.20}$$

such that $f_u, f_v, f_w \in H$. Here $f_u(x,y)$ and $f_v(x,y)$ are tangential force densities per unit depth.

From (2.17) we observe that the displacement vector $\mathbf{u}$ is fully determined by the functions u_1, v_1, and w_0. With this in mind, we proceed to derive the variational problem for the R3D plate model in terms of u_1, v_1, and w_0. Applying (2.18)-(2.20) to (2.12) and integrating with respect to z, the total potential energy of the plate is expressed as

$$\begin{aligned} \Pi(u_1,v_1,w_0) = \frac{1}{2}\int_\Omega \Big\{ & aI_3[(1-\nu)u_{1x}+\nu v_{1y}]u_{1x} \\ & + bI_3(u_{1y}+v_{1x})^2 + bI_1(u_1+w_{0x})^2 + bI_1(v_1+w_{0y})^2 \\ & + aI_3[\nu u_{1x}+(1-\nu)v_{1y}]v_{1y} + \kappa_u I_2 u_1^2 + \kappa_v I_2 v_1^2 \\ & + \kappa_w I_1 w_0^2 - 2[I_3(f_u u_1 + f_v v_1) + I_1 f_w w_0]\Big\}\,\mathrm{d}A\,. \end{aligned}$$

Utilizing the principle of the minimum total potential energy (2.13) with

$$\mathbf{\Phi} = z\phi_1(x,y)\mathbf{i} + z\psi_1(x,y)\mathbf{j} + \omega_0(x,y)\mathbf{k}\,, \tag{2.21}$$

where $\phi_1, \psi_1, \omega_0 \in V_0$, and decoupling the result into individual variational equations with respect to ϕ_1, ψ_1, and ω_0, we arrive to the following variational formulation of the R3D plate model.

$$\begin{aligned} \int_\Omega \Big\{ & aI_3[(1-\nu)u_{1x}+\nu v_{1y}]\phi_{1x} + bI_3(u_{1y}+v_{1x})\phi_{1y} \\ & + bI_1(u_1+w_{0x})\phi_1 + \kappa_u I_2 u_1\phi_1 - I_3 f_u\phi_1\Big\}\,\mathrm{d}A = 0\,, \end{aligned} \tag{2.22}$$

$$\begin{aligned} \int_\Omega \Big\{ & aI_3[\nu u_{1x}+(1-\nu)v_{1y}]\psi_{1y} + bI_3(u_{1y}+v_{1x})\psi_{1x} \\ & + bI_1(v_1+w_{0y})\psi_1 + \kappa_v I_2 v_1\psi_1 - I_3 f_v\psi_1\Big\}\,\mathrm{d}A = 0\,, \end{aligned} \tag{2.23}$$

$$\begin{aligned} \int_\Omega \Big\{ & bI_1(u_1+w_{0x})\omega_{0x} + bI_1(v_1+w_{0y})\omega_{0y} \\ & + \kappa_w I_1 w_0\omega_0\Big\}\,\mathrm{d}A - \int_\Sigma I_1 f_w\omega_0\,\mathrm{d}A = 0\,. \end{aligned} \tag{2.24}$$

Next, we summarize the variational formulations of the Mindlin and thin plate models. For the Mindlin plate model, in addition to the displacement relations (2.17), it is assumed that in (2.3),

$$\tau_{33} = 0 \tag{2.25}$$

implying

$$\varepsilon_{33} = \frac{-\nu}{1-\nu}(\varepsilon_{11}+\varepsilon_{22})\,.$$

Moreover, a shear correction factor $k_s > 0$ is introduced into the stress-strain relations (2.19) to account for the fact that shear strains are not constant over a

cross-section of the plate [13]:

$$\tau_{13} = k_s b(u_1 + w_{0x}), \quad \tau_{23} = k_s b(v_1 + w_{0y})\,.$$

Thus, the total potential energy of the plate is expressed as

$$\begin{aligned}\Pi(u_1, v_1, w_0) = \frac{1}{2}\int_\Omega \Big\{ &\hat{a} I_3[u_{1x}^2 + 2\nu v_{1y} u_{1x} + v_{1y}^2] \\ &+ bI_3(u_{1y} + v_{1x})^2 + k_s bI_1(u_1 + w_{0x})^2 + k_s bI_1(v_1 + w_{0y})^2 \\ &+ \kappa_u I_2 u_1^2 + \kappa_v I_2 v_1^2 + \kappa_w I_1 w_0^2 \\ &- 2[I_3(f_u u_1 + f_v v_1) + I_1 f_w w_0]\Big\}\,\mathrm{d}A\,.\end{aligned}$$

Applying the principle of the minimum total potential energy (2.13) with $\mathbf{\Phi}$ in the form (2.21) and decoupling the result into individual variations give the variational formulation of the Mindlin plate model as follows.

$$\begin{aligned}&\int_\Omega \Big\{ \hat{a} I_3[u_{1x} + \nu v_{1y}]\phi_{1x} + bI_3(u_{1y} + v_{1x})\phi_{1y} \\ &+ k_s bI_1(u_1 + w_{0x})\phi_1 + \kappa_u I_2 u_1 \phi_1 - I_3 f_u \phi_1 \Big\}\,\mathrm{d}A = 0\,, \\ &\int_\Omega \Big\{ \hat{a} I_3[\nu u_{1x} + v_{1y}]\psi_{1y} + bI_3(u_{1y} + v_{1x})\psi_{1x} \\ &+ k_s bI_1(v_1 + w_{0y})\psi_1 + \kappa_v I_2 v_1 \psi_1 - I_3 f_v \psi_1 \Big\}\,\mathrm{d}A = 0\,, \\ &\int_\Omega \Big\{ k_s bI_1(u_1 + w_{0x})\omega_{0x} + k_s bI_1(v_1 + w_{0y})\omega_{0y} \\ &+ \kappa_w I_1 w_0 \omega_0 - I_1 f_w \omega_0 \Big\}\,\mathrm{d}A = 0\,.\end{aligned}$$

For the thin plate model, it is further assumed that

$$\tau_{13} = \tau_{23} = 0\,. \tag{2.26}$$

This results in the conditions

$$\begin{aligned}u(x, y, z) &= -z w_{0x}(x, y) \\ v(x, y, z) &= -z w_{0y}(x, y) \\ w(x, y, z) &= w_0(x, y)\,.\end{aligned}$$

The total potential energy of the plate is now

$$\begin{aligned}\Pi(u_1, v_1, w_0) = \frac{1}{2}\int_\Omega \Big\{ &\hat{a} I_3[(w_{0xx} + w_{0yy})^2 + 2(1-\nu)(w_{0xy}^2 - w_{0xx} w_{0yy})] \\ &+ \kappa_u I_3 w_{0x}^2 + \kappa_v I_3 w_{0y}^2 + \kappa_w I_1 w_0^2 \\ &- 2[-I_3(f_u w_{0x} + f_v w_{0y}) + I_1 f_w w_0]\Big\}\,\mathrm{d}A\,.\end{aligned}$$

Again, according to (2.13) applied with (2.21), the variational formulation of the thin plate model is given by

$$\begin{aligned}&\int_\Omega \Big\{ \hat{a} I_3(w_{0xx} + w_{0yy})(\omega_{0xx} + \omega_{0yy}) + \kappa_u I_3 w_{0x}\omega_{0x} + \kappa_v I_3 w_{0y}\omega_{0y} \\ &+ \kappa_w I_1 w_0 \omega_0 - [-I_3(f_u \omega_{0x} + f_v \omega_{0y}) + I_1 f_w \omega_0]\Big\}\,\mathrm{d}A = 0\,,\end{aligned}$$

where we have used the following result obtained from Green's identities:

$$\int_\Omega \Big\{2w_{0xy}\omega_{0xy} - w_{0xx}\omega_{0yy} - \omega_{0xx}w_{0yy}\Big\}\,\mathrm{d}A = 0\,,$$

for any $\omega_0 \in H_0^2(\Omega)$.

3. Spatial approximation

In this section, spatially discretized plate models are determined from approximations of the variational formulations for the R3D, Mindlin, and thin plate distributed parameter models. The cubic B-spline finite element method with enforcement of zero Dirichlet boundary conditions corresponding to the assumption that the plate undergoes negligible displacement on the boundary Γ is used. These systems are central in formulating estimation problems in which data consists only of vertical displacements at points within Ω. Let

$$S^m(\Omega) = \{B_1, \ldots, B_m\} \tag{3.1}$$

be a set of linearly independent functions in $H^2(\Omega)$ from which we construct approximations to the solutions of the model equations. Define the column m-vector-valued function $\mathbf{B} : \Omega \mapsto \mathbb{R}^m$ by

$$\mathbf{B}(x,y) = [B_1(x,y), \ldots, B_m(x,y)]^T\,,$$

and express approximations of solutions u_1, v_1, and w_0 and the force densities f_u, f_v, and f_w as

$$\begin{aligned} u_1(x,y) &= \mathbf{B}(x,y)^T\bar{\mathbf{u}}_1 \\ v_1(x,y) &= \mathbf{B}(x,y)^T\bar{\mathbf{v}}_1 \\ w_0(x,y) &= \mathbf{B}(x,y)^T\bar{\mathbf{w}}_0 \end{aligned} \tag{3.2}$$

and

$$\begin{aligned} f_u(x,y) &= \mathbf{B}(x,y)^T\bar{\mathbf{f}}_u \\ f_v(x,y) &= \mathbf{B}(x,y)^T\bar{\mathbf{f}}_v \\ f_w(x,y) &= \mathbf{B}(x,y)^T\bar{\mathbf{f}}_w\,, \end{aligned} \tag{3.3}$$

where $\bar{\mathbf{u}}_1, \bar{\mathbf{v}}_1, \bar{\mathbf{w}}_0$, $\bar{\mathbf{f}}_u$, $\bar{\mathbf{f}}_v$, and $\bar{\mathbf{f}}_w$ are $m \times 1$ constant column vectors.

Substituting (3.2) and (3.3) into the variational formulation (2.22)-(2.24) of the R3D plate model leads to

$$\begin{aligned} &\Big\{\int_\Omega \big[aI_3(1-\nu)\mathbf{B}_x\mathbf{B}_x^T + bI_3\mathbf{B}_y\mathbf{B}_y^T + (bI_1+\kappa_u I_2)\mathbf{B}\mathbf{B}^T\big]\,\mathrm{d}A\Big\}\bar{\mathbf{u}}_1 \\ &+ \Big\{\int_\Omega \big[aI_3\nu\mathbf{B}_x\mathbf{B}_y^T + bI_3\mathbf{B}_y\mathbf{B}_x^T\big]\,\mathrm{d}A\Big\}\bar{\mathbf{v}}_1 \\ &+ \Big\{\int_\Omega bI_1\mathbf{B}\mathbf{B}_x^T\,\mathrm{d}A\Big\}\bar{\mathbf{w}}_0 = \Big\{\int_\Omega I_3\mathbf{B}\mathbf{B}^T\,\mathrm{d}A\Big\}\bar{\mathbf{f}}_u\,, \end{aligned} \tag{3.4}$$

$$\begin{aligned} &\Big\{\int_\Omega \big[aI_3\nu\mathbf{B}_y\mathbf{B}_x^T + bI_3\mathbf{B}_x\mathbf{B}_y^T\big]\,\mathrm{d}A\Big\}\bar{\mathbf{u}}_1 \\ &+ \Big\{\int_\Omega \big[aI_3(1-\nu)\mathbf{B}_y\mathbf{B}_y^T + bI_3\mathbf{B}_x\mathbf{B}_x^T + (bI_1+\kappa_v I_2)\mathbf{B}\mathbf{B}^T\big]\,\mathrm{d}A\Big\}\bar{\mathbf{v}}_1 \\ &+ \Big\{\int_\Omega bI_1\mathbf{B}\mathbf{B}_y^T\,\mathrm{d}A\Big\}\bar{\mathbf{w}}_0 = \Big\{\int_\Omega I_3\mathbf{B}\mathbf{B}^T\,\mathrm{d}A\Big\}\bar{\mathbf{f}}_v\,, \end{aligned} \tag{3.5}$$

$$\begin{aligned}
&\Big\{\int_\Omega bI_1\mathbf{B}_x\mathbf{B}^T\,\mathrm{d}A\Big\}\bar{\mathbf{u}}_1+\Big\{\int_\Omega \big[bI_1\mathbf{B}_y\mathbf{B}^T\big]\,\mathrm{d}A\Big\}\bar{\mathbf{v}}_1\\
&+\Big\{\int_\Omega \big[bI_1(\mathbf{B}_x\mathbf{B}_x^T+\mathbf{B}_y\mathbf{B}_y^T)+\kappa_w I_1\mathbf{B}\mathbf{B}^T\big]\,\mathrm{d}A\Big\}\bar{\mathbf{w}}_0\\
&=\Big\{\int_\Omega I_1\mathbf{B}\mathbf{B}^T\,\mathrm{d}A\Big\}\bar{\mathbf{f}}_w\,.
\end{aligned}\tag{3.6}$$

For the Mindlin plate model, we have similarly

$$\begin{aligned}
&\Big\{\int_\Omega \big[\hat{a}I_3\mathbf{B}_x\mathbf{B}_x^T+bI_3\mathbf{B}_y\mathbf{B}_y^T+(k_sbI_1+\kappa_uI_2)\mathbf{B}\mathbf{B}^T\big]\,\mathrm{d}A\Big\}\bar{\mathbf{u}}_1\\
&+\Big\{\int_\Omega \big[\hat{a}I_3\nu\mathbf{B}_x\mathbf{B}_y^T+bI_3\mathbf{B}_y\mathbf{B}_x^T\big]\,\mathrm{d}A\Big\}\bar{\mathbf{v}}_1\\
&+\Big\{\int_\Omega k_sbI_1\mathbf{B}\mathbf{B}_x^T\,\mathrm{d}A\Big\}\bar{\mathbf{w}}_0=\Big\{\int_\Omega I_3\mathbf{B}\mathbf{B}^T\,\mathrm{d}A\Big\}\bar{\mathbf{f}}_u\,,
\end{aligned}\tag{3.7}$$

$$\begin{aligned}
&\Big\{\int_\Omega \big[\hat{a}I_3\nu\mathbf{B}_y\mathbf{B}_x^T+bI_3\mathbf{B}_x\mathbf{B}_y^T\big]\,\mathrm{d}A\Big\}\bar{\mathbf{u}}_1\\
&+\Big\{\int_\Omega \big[\hat{a}I_3\mathbf{B}_y\mathbf{B}_y^T+bI_3\mathbf{B}_x\mathbf{B}_x^T+(k_sbI_1+\kappa_vI_2)\mathbf{B}\mathbf{B}^T\big]\,\mathrm{d}A\Big\}\bar{\mathbf{v}}_1\\
&+\Big\{\int_\Omega k_sbI_1\mathbf{B}\mathbf{B}_y^T\,\mathrm{d}A\Big\}\bar{\mathbf{w}}_0\\
&=\Big\{\int_\Omega I_3\mathbf{B}\mathbf{B}^T\,\mathrm{d}A\Big\}\bar{\mathbf{f}}_v\,,
\end{aligned}\tag{3.8}$$

$$\begin{aligned}
&\Big\{\int_\Omega k_sbI_1\mathbf{B}_x\mathbf{B}^T\,\mathrm{d}A\Big\}\bar{\mathbf{u}}_1+\Big\{\int_\Omega k_sbI_1\mathbf{B}_y\mathbf{B}^T\,\mathrm{d}A\Big\}\bar{\mathbf{v}}_1\\
&+\Big\{\int_\Omega k_sbI_1(\mathbf{B}_x\mathbf{B}_x^T+\mathbf{B}_y\mathbf{B}_y^T)+\kappa_wI_1\mathbf{B}\mathbf{B}^T\,\mathrm{d}A\Big\}\bar{\mathbf{w}}_0\\
&=\Big\{\int_\Omega I_1\mathbf{B}\mathbf{B}^T\,\mathrm{d}A\Big\}.\bar{\mathbf{f}}_w\,.
\end{aligned}\tag{3.9}$$

Finally, for the thin plate model, we obtain

$$\begin{aligned}
&\Big\{\int_\Omega \Big[\hat{a}I_3(\mathbf{B}_{xx}+\mathbf{B}_{yy})(\mathbf{B}_{xx}+\mathbf{B}_{yy})^T\\
&+I_3(\kappa_u\mathbf{B}_x\mathbf{B}_x^T+\kappa_v\mathbf{B}_y\mathbf{B}_y^T)+\kappa_wI_1\mathbf{B}\mathbf{B}^T\Big]\,\mathrm{d}A\Big\}\bar{\mathbf{w}}_0\\
&=\Big\{\int_\Omega -I_3\mathbf{B}_x\mathbf{B}^T\,\mathrm{d}A\Big\}\bar{\mathbf{f}}_u+\Big\{\int_\Omega -I_3\mathbf{B}_y\mathbf{B}^T\,\mathrm{d}A\Big\}\bar{\mathbf{f}}_v+\Big\{\int_\Omega I_1\mathbf{B}\mathbf{B}^T\,\mathrm{d}A\Big\}\bar{\mathbf{f}}_w\,.
\end{aligned}\tag{3.10}$$

To allow for the spatial variability of the coefficients and plate thickness, let $\{\Omega_k\}_{k=1}^N$ be a partition of Ω, $\Omega=\bigcup_k\Omega_k$, and define the functions

$$\Xi_k(x,y)=\begin{cases}1, & \text{when } (x,y)\in\Omega_k,\\ 0, & \text{when } (x,y)\notin\Omega_k\,.\end{cases}$$

We express the coefficients (2.6) and (2.16) and plate thickness h as linear combinations of Ξ_k of the form

$$\theta(x,y)=\sum_{k=1}^N\theta_k\Xi_k(x,y)$$

where θ represents a, $\hat{a}$, b, κ_u, κ_v, κ_w, or h, whichever is appropriate. Note that, for example,

$$h(x,y)a(x,y) = \sum_{k=1}^{N} h_k a_k \Xi_k(x,y)\,.$$

It is convenient to define the following matrices.

$$G_0^{(k)} = \int_\Omega \Xi_k \mathbf{B}\mathbf{B}^T \,\mathrm{d}A$$

with

$$G_0 = \sum_{k=1}^{N} G_0^{(k)} \quad \text{and} \quad G_{00}(\theta) = \sum_{k=1}^{N} \theta_k G_0^{(k)}\,,$$

and

$$\begin{gathered}
G_{x0}^{(k)} = \int_\Omega \Xi_k \mathbf{B}_x \mathbf{B}^T \,\mathrm{d}A, \quad G_{y0}^{(k)} = \int_\Omega \Xi_k \mathbf{B}_y \mathbf{B}^T \,\mathrm{d}A \\
G_{xx}^{(k)} = \int_\Omega \Xi_k \mathbf{B}_x \mathbf{B}_x^T \,\mathrm{d}A, \quad G_{yy}^{(k)} = \int_\Omega \Xi_k \mathbf{B}_y \mathbf{B}_y^T \,\mathrm{d}A \\
G_{xy}^{(k)} = \int_\Omega \Xi_k \mathbf{B}_x \mathbf{B}_y^T \,\mathrm{d}A \quad G_L^{(k)} = \int_\Omega \Xi_k (\mathbf{B}_{xx} + \mathbf{B}_{yy})(\mathbf{B}_{xx}^T + \mathbf{B}_{yy}^T) \,\mathrm{d}A
\end{gathered}$$

with

$$\begin{gathered}
G_{x0}(\theta) = \sum_{k=1}^{N} \theta_k G_{x0}^{(k)}, \quad G_{y0}(\theta) = \sum_{k=1}^{N} \theta_k G_{y0}^{(k)} \\
G_{xx}(\theta) = \sum_{k=1}^{N} \theta_k G_{xx}^{(k)}, \quad G_{yy}(\theta) = \sum_{k=1}^{N} \theta_k G_{yy}^{(k)} \\
G_{xy}(\theta) = \sum_{k=1}^{N} \theta_k G_{xy}^{(k)}, \quad G_L(\theta) = \sum_{k=1}^{N} \theta_k G_L^{(k)}\,,
\end{gathered}$$

where we express dependence on the coefficients when necessary. Finally, with reference to (3.4)-(3.6), (3.7)-(3.9), and (3.10), we define the following matrices for the R3D plate, Mindlin plate, and the thin plate models, respectively. For ease of exposition, subscripts R, M, and T will refer to the respective plate models. For the R3D plate model, we introduce the matrices

$$\begin{aligned}
G_{R11} &= G_{xx}((1-\nu)I_3 a) + G_{yy}(I_3 b) + G_{00}(I_1 b) + G_{00}(I_2 \kappa_u) \\
G_{R12} &= G_{xy}(\nu I_3 a) + G_{yx}(I_3 b) \\
G_{R13} &= G_{0x}(I_1 b) \\
G_{R22} &= G_{yy}((1-\nu)I_3 a) + G_{xx}(I_3 b) + G_{00}(I_1 b) + G_{00}(I_2 \kappa_v) \\
G_{R23} &= G_{0y}(I_1 b) \\
G_{R33} &= G_{xx}(I_1 b) + G_{yy}(I_1 b)\,.
\end{aligned} \tag{3.11}$$

For the Mindlin plate model, we define the matrices

$$\begin{aligned}
G_{M11} &= G_{xx}(I_3\hat{a}) + G_{yy}(I_3 b) + k_s G_{00}(I_1 b) + G_{00}(I_2\kappa_u)\\
G_{M12} &= G_{xy}(\nu I_3\hat{a}) + G_{yx}(I_3 b)\\
G_{M13} &= k_s G_{0x}(I_1 b)\\
G_{M22} &= G_{yy}(I_3\hat{a}) + G_{xx}(I_3 b) + k_s G_{00}(I_1 b) + G_{00}(I_2\kappa_v)\\
G_{M23} &= k_s G_{0y}(I_1 b)\\
G_{M33} &= k_s G_{xx}(I_1 b) + k_s G_{yy}(I_1 b)\,.
\end{aligned} \tag{3.12}$$

For the thin plate, we assign the matrix

$$H_T = G_L(I_3\hat{a}) + G_{xx}(I_3\kappa_u) + G_{yy}(I_3\kappa_v) + G_{00}(I_1\kappa_w)\,. \tag{3.13}$$

Of course, terms may be written as multipliers of the matrices in the case of constant thickness, Young's modulus, and Poisson's ratio. Applying (3.11) to (3.4)-(3.6) renders the following system for the R3D plate model.

$$\begin{aligned}
G_{R11}\bar{\mathbf{u}}_{R1} + G_{R12}\bar{\mathbf{v}}_{R1} + G_{R13}\bar{\mathbf{w}}_{R0} &= G_0(I_3)\bar{\mathbf{f}}_{Ru}\\
G_{R12}^T\bar{\mathbf{u}}_{R1} + G_{R22}\bar{\mathbf{v}}_{R1} + G_{R23}\bar{\mathbf{w}}_{R0} &= G_0(I_3)\bar{\mathbf{f}}_{Rv}\\
G_{R13}^T\bar{\mathbf{u}}_{R1} + G_{R23}^T\bar{\mathbf{v}}_{R1} + G_{R33}\bar{\mathbf{w}}_{R0} &= G_0(I_1)\bar{\mathbf{f}}_{Rw}\,.
\end{aligned}$$

Similarly, applying (3.12) to (3.7)-(3.9), for the Mindlin plate model we obtain the system

$$\begin{aligned}
G_{M11}\bar{\mathbf{u}}_{M1} + G_{M12}\bar{\mathbf{v}}_{M1} + G_{M13}\bar{\mathbf{w}}_{M0} &= G_0(I_3)\bar{\mathbf{f}}_{Mu}\,,\\
G_{M12}^T\bar{\mathbf{u}}_{M1} + G_{M22}\bar{\mathbf{v}}_{M1} + G_{M23}\bar{\mathbf{w}}_{M0} &= G_0(I_3)\bar{\mathbf{f}}_{Mv}\,,\\
G_{M13}^T\bar{\mathbf{u}}_{M1} + G_{M23}^T\bar{\mathbf{v}}_{M1} + G_{M33}\bar{\mathbf{w}}_{M0} &= G_0(I_1)\bar{\mathbf{f}}_{Mw}\,.
\end{aligned}$$

Observe that the R3D and Mindlin systems have the form

$$\begin{aligned}
G_{*11}\bar{\mathbf{u}}_{*1} + G_{*12}\bar{\mathbf{v}}_{*1} + G_{*13}\bar{\mathbf{w}}_{*0} &= G_0(I_3)\bar{\mathbf{f}}_{*u}\,,\\
G_{*12}^T\bar{\mathbf{u}}_{*1} + G_{*22}\bar{\mathbf{v}}_{*1} + G_{*23}\bar{\mathbf{w}}_{*0} &= G_0(I_3)\bar{\mathbf{f}}_{*v}\,,\\
G_{*13}^T\bar{\mathbf{u}}_{*1} + G_{*23}^T\bar{\mathbf{v}}_{*1} + G_{*33}\bar{\mathbf{w}}_{*0} &= G_0(I_1)\bar{\mathbf{f}}_{*w}\,,
\end{aligned} \tag{3.14}$$

where $* = R$ or M, whichever is appropriate.

Next, we wish to derive the expressions for $\bar{\mathbf{w}}_{*0}$ in terms of $\bar{\mathbf{f}}_{*u}$, $\bar{\mathbf{f}}_{*v}$, and $\bar{\mathbf{f}}_{*w}$. To this end, we introduce the matrices

$$\begin{aligned}
H_{*11} &= G_{*22} - G_{*12}^T G_{*11}^{-1} G_{*12}\\
H_{*12} &= G_{*23} - G_{*12}^T G_{*11}^{-1} G_{*13}\\
H_{*22} &= G_{*33} - G_{*13}^T G_{*11}^{-1} G_{*13}\\
H_{*} &= H_{*22} - H_{*12}^T H_{*11}^{-1} H_{*12}
\end{aligned}$$

and vectors

$$\tilde{\mathbf{f}}_{*v} = G_0(I_3)\bar{\mathbf{f}}_{*v} - G_{*12}^T G_{*11}^{-1} G_0(I_3)\bar{\mathbf{f}}_{*u}\,, \tag{3.15}$$

$$\tilde{\mathbf{f}}_{*w} = G_0(I_1)\bar{\mathbf{f}}_{*w} - G_{*13}^T G_{*11}^{-1} G_0(I_3)\bar{\mathbf{f}}_{*u}\,. \tag{3.16}$$

Then the solution of (3.14) may then be expressed as

$$H_*\bar{\mathbf{w}}_{*0} = \tilde{\mathbf{f}}_{*w} - H_{*12}^T H_{*11}^{-1}\tilde{\mathbf{f}}_{*v}\,, \tag{3.17}$$

$$H_{*11}\bar{\mathbf{v}}_{*1} = \tilde{\mathbf{f}}_{*v} - H_{*12}\bar{\mathbf{w}}_{*0}\,, \tag{3.18}$$

$$G_{*11}\bar{\mathbf{u}}_{*1} = G_0(I_3)\bar{\mathbf{f}}_{*u} - G_{*12}\bar{\mathbf{v}}_{*1} - G_{*13}\bar{\mathbf{w}}_{*0}\,. \tag{3.19}$$

Applying (3.15) and (3.16) to (3.17), we obtain the following expression for $\bar{\mathbf{w}}_{*0}$ for the R3D and the Mindlin plate models,

$$\begin{aligned} H_*\bar{\mathbf{w}}_{*0} = &\big(H_{*12}^T H_{*11}^{-1} G_{*12}^T - G_{*13}^T\big) G_{*11}^{-1} G_0(I_3)\bar{\mathbf{f}}_{*u} \\ &- H_{*12}^T H_{*11}^{-1} G_0(I_3)\bar{\mathbf{f}}_{*v} + G_0(I_1)\bar{\mathbf{f}}_{*w}\,. \end{aligned} \tag{3.20}$$

From (3.10) and (3.13), for the thin plate model we have

$$H_T\bar{\mathbf{w}}_{T0} = G_{x0}(I_3)\bar{\mathbf{f}}_{Tu} + G_{y0}(I_3)\bar{\mathbf{f}}_{Tv} + G_0(I_1)\bar{\mathbf{f}}_{Tw}\,. \tag{3.21}$$

4. Estimation of parameters

In this section, we consider the estimation of body force densities, plate thickness, and elastic foundation stiffness parameters based on vertical displacement data. Specifically, we assume that data of the vertical displacements z_i at points $(x_i, y_i) \in \Omega$ for $i = 1, \dots, N_o$ are given. The first problem is to estimate the force density components $\bar{\mathbf{f}}_u$, $\bar{\mathbf{f}}_v$, and $\bar{\mathbf{f}}_w$ under the assumption that the values of plate thickness h and elastic foundation stiffness parameters κ_u, κ_v, and κ_w are specified.

A related problem is the interpolation problem [26, 35] that seeks a function $z(x, y)$ defined for $(x, y) \in \Omega$ such that $z(x_i, y_i) = z_i$. Towards this end, we express the function z as

$$z(x, y) = \mathbf{B}(x, y)^T\bar{\mathbf{z}}\,,$$

where the components of $\mathbf{B}(x, y)$ are a set of linearly independent functions in S^m (3.1). We seek to determine the m-vector $\bar{\mathbf{z}}$ to minimize the error functional

$$E_I(\bar{\mathbf{z}}) = \sum_{i=1}^{N_o} (\mathbf{B}(x_i, y_i)^T\bar{\mathbf{z}} - z_i)^2\,.$$

Define the interpolation matrix

$$J = \sum_{i=1}^{N_o} \mathbf{B}(x_i, y_i)\mathbf{B}(x_i, y_i)^T$$

and the vector

$$\bar{\boldsymbol{\zeta}} = \sum_{i=1}^{N_o} z_i\mathbf{B}(x_i, y_i)\,.$$

Under the assumption that the data is sufficient that J is invertible, the interpolating function obtained for the data (x_i, y_i, z_i) is given by

$$z(x, y) = \mathbf{B}(x, y)^T J^{-1}\bar{\boldsymbol{\zeta}} \tag{4.1}$$

The objective is to use the interpolating function (4.1) in conjunction with the plate models to obtain information on the body force densities. The underlying assumption is that the vertical displacement and the forces densities are independent of the model. Accordingly, we set

$$w_0(x, y) = z(x, y)$$

Hence, with

$$w_0(x, y) = \mathbf{B}(x, y)^T\bar{\mathbf{w}}_0$$

it follows from linear independence of the components of $\mathbf{B}(x, y)$ that

$$\bar{\mathbf{w}}_0 = J^{-1}\bar{\boldsymbol{\zeta}}\,.$$

With reference to (3.20) and (3.21), we define the matrices

$$\begin{aligned} N_{*u} &= \big(H_{*12}^T H_{*11}^{-1} G_{*12}^T - G_{*13}^T\big) G_{*11}^{-1} G_0(I_3) \\ N_{*v} &= -H_{*12}^T H_{*11}^{-1} G_0(I_3) \\ N_{Tu} &= G_{x0}(I_3) \\ N_{Tv} &= G_{y0}(I_3)\,. \end{aligned}$$

Then the relations (3.20) and (3.21) yield the following set of constraining equations among the quantities $\bar{\mathbf{w}}_0$, $\bar{\mathbf{f}}_u$, $\bar{\mathbf{f}}_v$, and $\bar{\mathbf{f}}_w$.

$$N_{Tu}\bar{\mathbf{f}}_u + N_{Tv}\bar{\mathbf{f}}_v + G_0(I_1)\bar{\mathbf{f}}_w = H_T\bar{\mathbf{w}}_0\,, \tag{4.2}$$

$$N_{Mu}\bar{\mathbf{f}}_u + N_{Mv}\bar{\mathbf{f}}_v + G_0(I_1)\bar{\mathbf{f}}_w = H_M\bar{\mathbf{w}}_0\,, \tag{4.3}$$

$$N_{Ru}\bar{\mathbf{f}}_u + N_{Rv}\bar{\mathbf{f}}_v + G_0(I_1)\bar{\mathbf{f}}_w = H_R\bar{\mathbf{w}}_0\,. \tag{4.4}$$

Remark 4.1. Under the assumption that the tangential forces are relatively small, setting

$$\bar{\mathbf{f}}_u = \bar{\mathbf{f}}_v = 0 \tag{4.5}$$

from (4.2)-(4.4) for the thin plate, the Mindlin plate, and the R3D plate models, respectively, we have

$$\bar{\mathbf{f}}_{*w} = [G_0(I_1)]^{-1} H_*\bar{\mathbf{w}}_0\,, \tag{4.6}$$

where $*$ stands for T, M, and R, respectively.

Equation (4.6) will be used in Section 5 to compare numerical estimates of normal force densities produced by each of the three plate models under assumption that the tangential external body force is zero.

Continuing on subtracting (4.2) from (4.3) and (4.4) and defining the matrices

$$\begin{aligned} L_{Mu} &= N_{Mu} - N_{Tu}, \quad L_{Mv} = N_{Mv} - N_{Tv} \\ L_{Ru} &= N_{Ru} - N_{Tu}, \quad L_{Rv} \ = N_{Rv} - N_{Tv}\,, \end{aligned}$$

we have

$$L_{Mu}\bar{\mathbf{f}}_u + L_{Mv}\bar{\mathbf{f}}_v = (H_M - H_T)\bar{\mathbf{w}}_0 \tag{4.7}$$

$$L_{Ru}\bar{\mathbf{f}}_u + L_{Rv}\bar{\mathbf{f}}_v = (H_R - H_T)\bar{\mathbf{w}}_0 \tag{4.8}$$

as conditions from the models to constrain the in-plane body force densities $\bar{\mathbf{f}}_u$ and $\bar{\mathbf{f}}_v$.

In practice, system (4.7) and (4.8) often involves ill-conditioned matrices. To overcome this obstacle, we seek a solution $(\bar{\mathbf{f}}_u, \bar{\mathbf{f}}_v)$ of (4.7) and (4.8) by minimizing the quadratic error functional

$$\begin{aligned} E(\bar{\mathbf{f}}_u, \bar{\mathbf{f}}_v) &= \sigma_M \|L_{Mu}\bar{\mathbf{f}}_u + L_{Mv}\bar{\mathbf{f}}_v - (H_M - H_T)\bar{\mathbf{w}}_0\|^2 \\ &\quad + \sigma_R \|L_{Ru}\bar{\mathbf{f}}_u + L_{Rv}\bar{\mathbf{f}}_v - (H_R - H_T)\bar{\mathbf{w}}_0\|^2 \\ &\quad + \sigma_u \|\bar{\mathbf{f}}_u\|^2 + \sigma_v \|\bar{\mathbf{f}}_v\|^2\,, \end{aligned} \tag{4.9}$$

where σ_M, σ_R, σ_u, and σ_v are positive weights to be chosen to reflect estimates of the precision of the corresponding term. For example, in computations in Section 5, we weight the variances for the R3D and the Mindlin the same by choosing σ_R and σ_M both equal 1 while σ_u and σ_v both equal to 10^{-16} to reflect the previous estimates when $\bar{\mathbf{f}}_u$ and $\bar{\mathbf{f}}_v$ were assumed to be zero.

Remark 4.2. The R3D plate, Mindlin plate, and thin plate models form a hierarchy of plate models based on assumptions imposed on stresses. The R3D plate model represents the most generalized (top) plate model with the only assumption on stresses given by the stress-strain relation (2.3). The R3D plate model is followed by the Mindlin plate model that carries zero transverse normal stress assumption (2.25). The Mindlin plate model is in turn followed by the thin plate model that imposes additional assumption that transverse shear stresses are negligible (2.26). With this in mind, the estimates (4.6) obtained under constraint (4.5) can be considered as prior information from each individual plate model. Then the minimization of $E(\bar{\mathbf{f}}_u, \bar{\mathbf{f}}_v)$ corresponds to finding the maximum likelihood estimator of a probability density function that includes priors from the individual plate models.

Next, we introduce the matrices

$$\begin{aligned} L_{uu} &= \sigma_M L_{Mu}^T L_{Mu} + \sigma_R L_{Ru}^T L_{Ru} + \sigma_u I \\ L_{vv} &= \sigma_M L_{Mv}^T L_{Mv} + \sigma_R L_{Rv}^T L_{Rv} + \sigma_v I \\ L_{uv} &= \sigma_M L_{Mu}^T L_{Mv} + \sigma_R L_{Ru}^T L_{Rv}\,, \end{aligned}$$

where I is the identity matrix, and the vectors

$$\begin{aligned} \mathbf{W}_u^T &= \sigma_M \big[(H_M - H_T)\bar{\mathbf{w}}_0\big]^T L_{Mu} + \sigma_R \big[(H_R - H_T)\bar{\mathbf{w}}_0\big]^T L_{Ru} \\ \mathbf{W}_v^T &= \sigma_M \big[(H_M - H_T)\bar{\mathbf{w}}_0\big]^T L_{Mv} + \sigma_R \big[(H_R - H_T)\bar{\mathbf{w}}_0\big]^T L_{Rv} \end{aligned}$$

With the above notation, the error functional (4.9) takes the form

$$E(\bar{\mathbf{f}}_u, \bar{\mathbf{f}}_v) = \bar{\mathbf{f}}_u^T L_{uu} \bar{\mathbf{f}}_u + 2\bar{\mathbf{f}}_u^T L_{uv} \bar{\mathbf{f}}_v + \bar{\mathbf{f}}_v^T L_{vv} \bar{\mathbf{f}}_v - 2\big[\mathbf{W}_u^T \bar{\mathbf{f}}_u + \mathbf{W}_v^T \bar{\mathbf{f}}_v\big] + E(0,0)\,.$$

The minimizer $(\bar{\mathbf{f}}_u, \bar{\mathbf{f}}_v)$ of E satisfies the normal equations

$$\begin{aligned} L_{uu}\bar{\mathbf{f}}_u + L_{uv}\bar{\mathbf{f}}_v &= \mathbf{W}_u \\ L_{uv}^T\bar{\mathbf{f}}_u + L_{vv}\bar{\mathbf{f}}_v &= \mathbf{W}_v \end{aligned}$$

which yield

$$\begin{aligned} \bar{\mathbf{f}}_v &= \big[L_{vv} - L_{uv}^T L_{uu}^{-1} L_{uv}\big]^{-1}\big(\mathbf{W}_v - L_{uv}^T L_{uu}^{-1}\mathbf{W}_u\big) \\ \bar{\mathbf{f}}_u &= L_{uu}^{-1}\big(\mathbf{W}_u - L_{uv}\bar{\mathbf{f}}_v\big)\,. \end{aligned}$$

Equations (4.2)-(4.4) now render

$$\bar{\mathbf{f}}_{*w} = [G_0(I_1)]^{-1}\big(H_*\bar{\mathbf{w}}_0 - N_{*u}\bar{\mathbf{f}}_u - N_{*v}\bar{\mathbf{f}}_v\big)\,, \tag{4.10}$$

where $*$ corresponds to T, M, and R, respectively. Estimates for $\bar{\mathbf{u}}_{*1}$ and $\bar{\mathbf{v}}_{*1}$ are obtained by means of equations (3.15)-(3.19). Using (3.2), we obtain the tangential components of displacement, and from the stress-displacement relations (2.19) of the R3D plate model we obtain strain estimates. Finally, we make the following observation.

Remark 4.3. The continuous dependence of force densities, displacements, and stresses on parameters h, κ_u, κ_v, and κ_w follows from the algebraic expressions satisfied by the matrices and vectors in the above.

Remark 4.4. Expressions for estimates of of body force densities, displacements, and stresses are obtained from normal displacement data given plate thickness h and foundation stiffness parameters κ_u, κ_v, and κ_w under the assumption that

the body force density components are independent of the model. The three model equations are used in essence to solve simultaneously for $\bar{\mathbf{f}}_u$ and $\bar{\mathbf{f}}_v$. Different models then yield different estimates for the normal body force density component $\bar{\mathbf{f}}_w$, even though the estimates may be quite close for certain values of h, κ_u, κ_v, κ_w (see, for instance, the numerical example in Section 5).

Next, we consider the estimation of the plate thickness h and foundation stiffness parameters κ_u, κ_v, and κ_w under the assumption that the estimations of $\bar{\mathbf{f}}_w$ from different plate models should be close. To that end, we set $q = (h, \kappa_u, \kappa_v, \kappa_w)$ and proceed, for simplicity, as though they are constants. The case in which the parameters are variable is similar.

Let $Q \subset \mathbb{R}^4$ be a set of admissible parameters q. We consider the cost functional measuring the total difference between the estimates of $\bar{\mathbf{f}}_w$ from pairs of different plate models in the form

$$\begin{aligned} J_c(q) = \xi_{RT}\|\bar{\mathbf{f}}_{Rw}(q) - \bar{\mathbf{f}}_{Tw}(q)\| + \xi_{MT}\|\bar{\mathbf{f}}_{Mw}(q) - \bar{\mathbf{f}}_{Tw}(q)\| \\ + \xi_{RM}\|\bar{\mathbf{f}}_{Rw}(q) - \bar{\mathbf{f}}_{Mw}(q)\| \end{aligned} \tag{4.11}$$

and seek the value $q^* \in Q$ minimizing the above functional. The estimates $\bar{\mathbf{f}}_{*w}(q)$, with $* = R$, T, and M, are obtained from (4.10), and the positive weights ξ_{RT}, ξ_{MT}, and ξ_{RM} are chosen to emphasize a particular model. Typically, we choose $\xi_{RT} = \xi_{MT} = \xi_{RM}$.

The physical meaning of parameters q suggests that Q is compact in $\mathbb{R}^4$. Therefore, from continuity of the mapping given in terms of the functional (4.11), there exists the minimizer of $J_c(q)$. In the next section we present the results for this minimization.

5. Numerical example

We present a numerical example motivated by the geoscience application of deformation associated with shallow, sill-like magma intrusions (laccolith formation). A classic and well-studied example of laccolith formation is the Henry Mountains, UT, the last-named mountain range in the continental USA. The Henry Mountains were formed by a complex of shallow intrusions 28-25 million years ago [22] at 1.5-2 km depths. Deformation of overlying sandstone layers by the intrusions is well documented due to erosion into the tops of the intrusions (see, for example [10]). The vertical displacement data are obtained from the structure contour map of Hunt et al. [8] for Mt. Holmes and Mt. Ellsworth in Henry Mountains, noting the top-most ∼100 m is interpolated. Mt. Holmes and Mt. Ellsworth topographic map and Henry Mountains structure contour map with interpolated top are presented in Figure 1 (A) and (B), respectively.

The plate thickness h, size of the domain Ω, and elastic parameters E and ν are given as geophysically reasonable numbers. The foundation stiffness parameters κ_u, κ_v, and κ_w and the shear correction factor k_s are specified through numerical experience. For the sake of simplicity we assume $\kappa_u = \kappa_v = \kappa_w$ and suppress subscripts u, v, and w. The values of parameters used in the example are summarized in Table 1.

To develop a spatial approximation, we consider $\Omega = (0, L_x) \times (0, L_y)$. For the approximation basis functions we use products of cubic B-splines defined on uniform partition on $(0, L_x)$ and $(0, L_y)$, with n_x and n_y subintervals, respectively

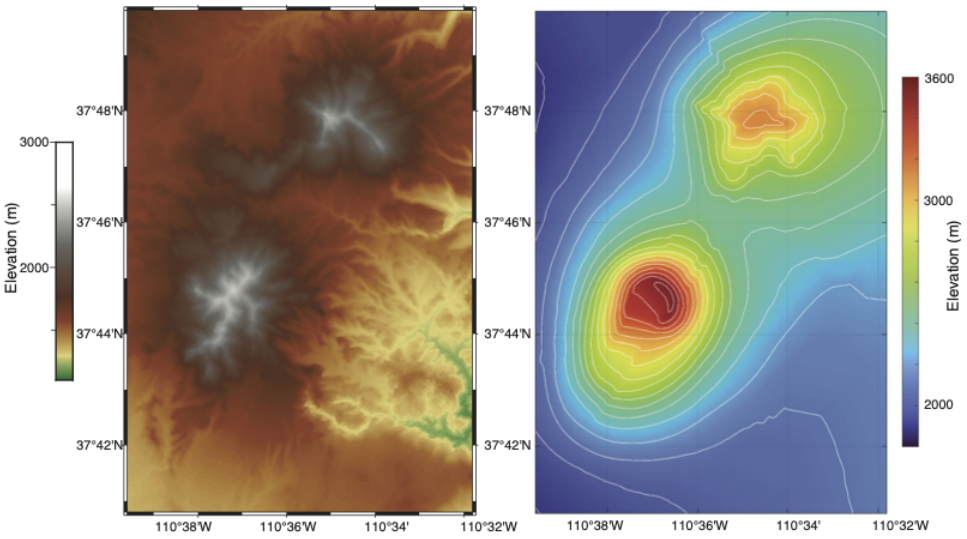

(A) (B)

FIGURE 1. (A) Topographic map of Mt. Holmes (top) and Mt. Ellsworth (bottom), Henry Mountains, UT. (B) Structure contour map with interpolated top-most ∼100 m (B).

TABLE 1. Values of parameters used in the example

Plate horizontal dimensions	$L_x = 14,600$ m, $L_y = 15,000$ m
Number of subintervals of partitions	$n_x = n_y = 12$
Plate thickness	$h = 1400$ m
Young's modulus	$E = 1.0 \times 10^9$ Pa
Poisson's ratio	$\nu = 0.25$
Foundation stiffness parameter	$\kappa = 10^5$ N/m^3
Shear correction factor	$k_s = 1$
Weights of the models	$\sigma_M = \sigma_R = 1$, $\sigma_u = \sigma_v = 10^{-16}$ $\xi_{RT} = \xi_{MT} = \xi_{RT} = 1$

[26]. Accordingly, let $b_i^{(x)}(x)$, for $i = 1, \ldots, m_x = n_x + 3$ and $b_i^{(y)}(y)$, for $i = 1, \ldots, m_y = n_y + 3$ denote cubic B-splines defined with respect to the meshes. In addition, define the m_x- and m_y-column-vector-valued functions by

$$\mathbf{b}^{(x)}(x) = [b_1^{(x)}(x), \ldots, b_{m_x}^{(x)}(x)]^T$$
$$\mathbf{b}^{(y)}(y) = [b_1^{(y)}(y), \ldots, b_{m_y}^{(y)}(y)]^T$$

Finally, define the $m = m_x m_y$-column vector as the tensor product of $\mathbf{b}^{(x)}$ and $\mathbf{b}^{(y)}$

$$B(x, y) = \mathbf{b}^{(x)}(x) \otimes \mathbf{b}^{(y)}(y)$$

Results in the graphs are presented on the domain $(0, 10^4) \times (0, 1.5 \times 10^4)$ m^2 to account for edge affects. The estimates of the scalar components of displacements and force densities are obtained from (3.2) and (3.3). As before, the subscripts R, M, and T stand for the R3D, Mindlin, and thin plate model, respectively. Uplift data are given at (x, y) locations over the domain, and the Henry Mountains surface data are shown in Figure 2(A).

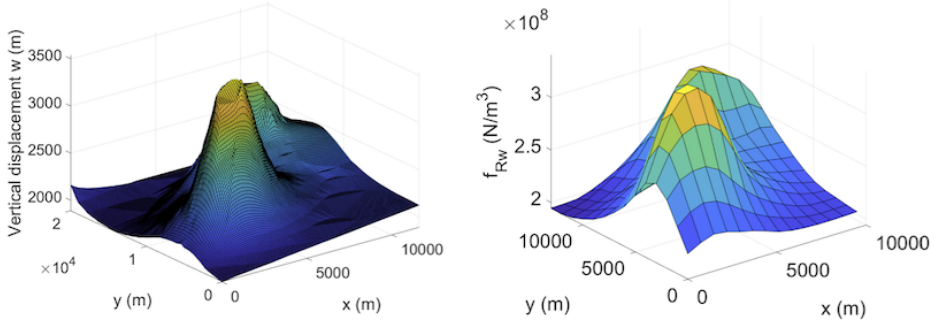

(A) (B)

FIGURE 2. (A) Henry Mountains surface data. (B) Force density f_{Rw} estimated from the R3D plate model with $f_u = f_v = 0$.

The graph of the normal body force density f_{Rw} using the R3D plate model with $f_u = f_v = 0$ is portrayed in Figure 2(B). The estimates of $\bar{\mathbf{f}}_{Rw}$ are calculated from (4.10). For comparison with the thin plate and Mindlin plate models, relative differences in estimates of f_w from different models are given below in which the absolute difference is normalized by the H-norm of f_{Rw}.

$$\frac{\|f_{Rw} - f_{Tw}\|_H}{\|f_{Rw}\|_H} = 1.44\times10^{-4}$$
$$\frac{\|f_{Mw} - f_{Tw}\|_H}{\|f_{Rw}\|_H} = 1.43\times10^{-4}$$
$$\frac{\|f_{Rw} - f_{Mw}\|_H}{\|f_{Rw}\|_H} = 7.88\times10^{-6}\,.$$

The estimated tangential body force densities per unit depth, f_u and f_v, obtained from the family of the three plate models are presented in Figures 3 (A) and (B), respectively. The corresponding values of $\bar{\mathbf{f}}_u$ and $\bar{\mathbf{f}}_v$ are minimizers of the error functional (4.9). One can observe that both f_u and f_v are relatively small compared to the result for f_{Rw} as to be expected. Given the estimated f_u and f_v, the normal force density f_w may be estimated from the equations (4.10) for each plate model. Figure 3(C) represents the normal force density f_{Rw} obtained from (4.10) using the R3D plate model. As one can observe from the graphs in Figures 2(B) and 3(C), the estimates of f_{Rw} with and without assumption that $f_u = f_v = 0$ are quite close, since f_u and f_v are relatively small for the values of model parameters used in this example. The graph of the relative difference between the f_{Rw} estimated from the family of three plate models without assumption $f_u = f_v = 0$ and f_{Rw} obtained from the R3D plate model under the assumption $f_u = f_v = 0$ is given in Figure 3(D).

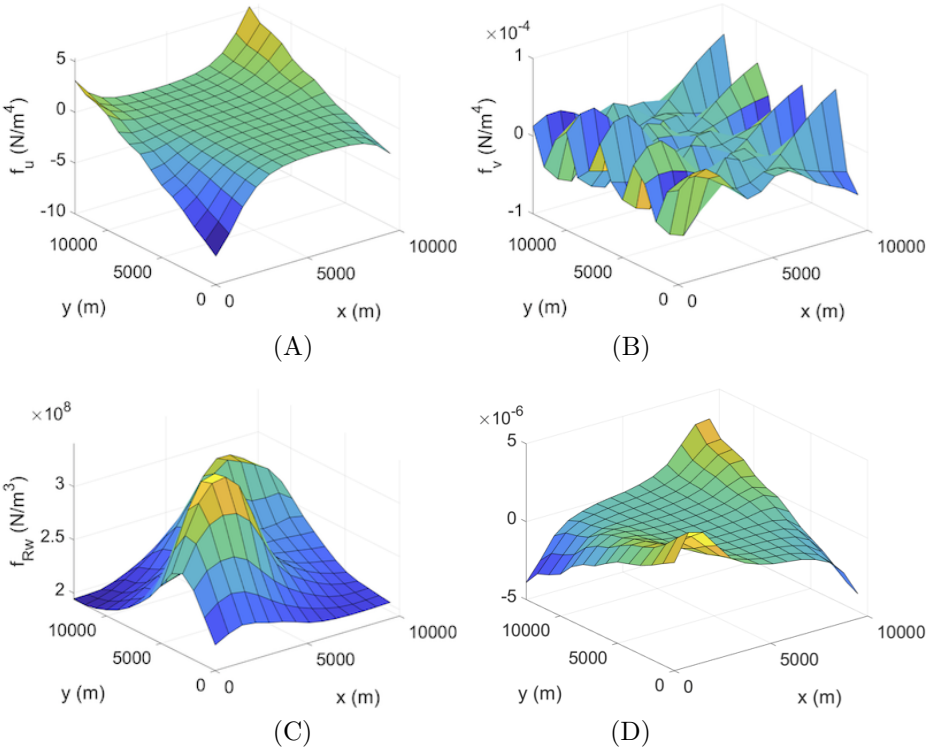

FIGURE 3. Force densities estimated from the family of plate models: (A) Force density per unit depth, f_u. (B) Force density per unit depth, f_v. (C) Force density f_{Rw}. (D) Relative difference between f_{Rw} in Figures 2 (B) and 3 (C).

For comparison with the thin and Mindlin plate models, below we present relative differences in estimates of f_w calculated from (4.10) for different models without assumption that $f_u = f_v = 0$.

$$\frac{\|f_{Rw} - f_{Tw}\|_H}{\|f_{Rw}\|_H} = 2.7{\times}10^{-3}$$
$$\frac{\|f_{Mw} - f_{Tw}\|_H}{\|f_{Rw}\|_H} = 3.0{\times}10^{-3}$$
$$\frac{\|f_{Rw} - f_{Mw}\|_H}{\|f_{Rw}\|_H} = 3.53{\times}10^{-4}\,.$$

Figures 4 (A) and (B) show the estimated tangential displacement components u and v obtained from (3.15)-(3.19) for the R3D plate model. Here the tangential force densities per unit depth, f_u and f_v, are estimated from the family of three plate models and f_w is calculated from (4.10) for the R3D plate model. The values of u and v estimated from the R3D plate model are used to calculate the transverse shear and normal stresses τ_{13}, τ_{23}, and τ_{33} from the strain-displacement and stress-strain relations (2.2) and (2.3), respectively. The calculation results are pictured in Figures 4 (C)–(E).

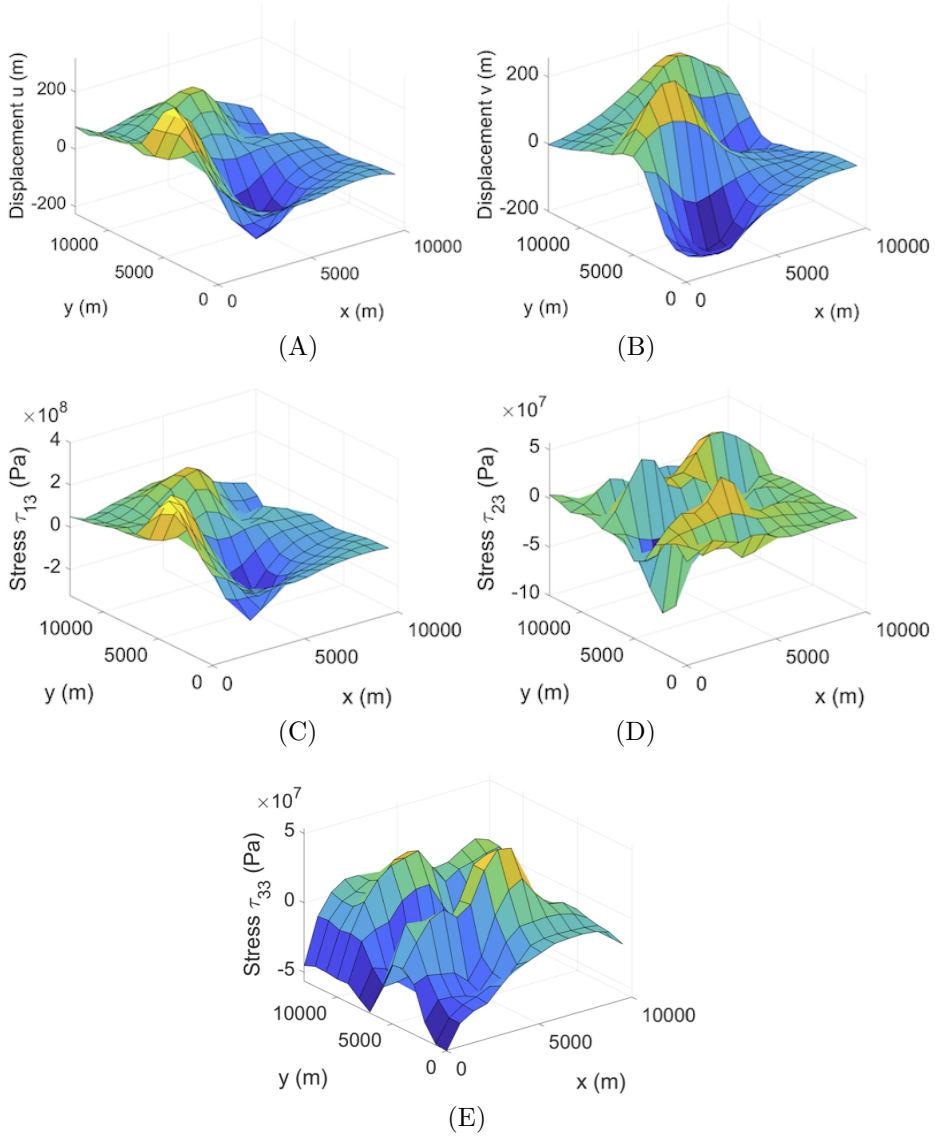

FIGURE 4. Displacements and stresses estimated from the R3D plate model with f_u and f_v estimated from the family of plate models and subsequent estimation of f_w from the R3D plate model: (A) Displacement u. (B) Displacement v. (C) Stress τ_{13}. (D) Stress τ_{23}. (E) Stress τ_{33}.

Figure 5(A) represents the level curves of the cost functional J_c (4.11) measuring total difference between the estimates of the normal force density f_w from the pairs of different plate models as a function of parameters $q = (h, \kappa)$. The direct evaluation of J_c gives the unique global minimum, with respect to the chosen evaluation mesh, at $h = 2000$ m and $\kappa = 3 \times 10^6$ N/m^3. Figure 5(B) shows the absolute

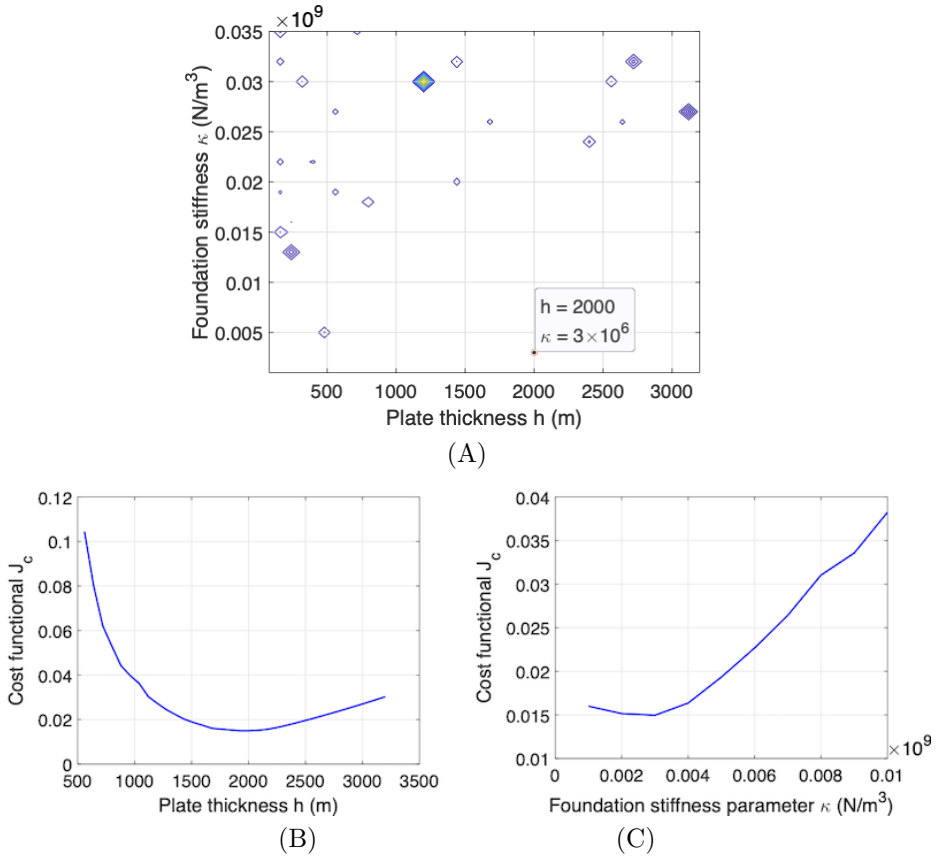

FIGURE 5. Optimal values of the plate thickness h and the foundation stiffness parameter κ: (A) The level curves of the cost functional $J_c(h, \kappa)$. (B) Cost functional J_c as a function of h with optimal $\kappa = 3 \times 10^6$ N/m^3. (C) Cost functional J_c as a function of κ with optimal $h = 2000$ m.

value of the cost functional J_c as a function of h, while the foundation stiffness parameter κ is fixed at the optimal value 3×10^6 N/m^3. Figure 5(C) represents the absolute value of the cost functional J_c as a function of κ, with the optimal plate thickness $h = 2000$ m fixed. For easy representation, in Figures 5 (B) and (C), the value of the cost functional J_c is rescaled by dividing its absolute value by Young's modulus E. According to Jackson and Pollard [10], the intrusions exposed in the Henry Mountains were emplaced at ∼2-4 km depth. In [22], the estimated depth of the intrusion is ∼1.5-2 km. Work [5] that employs a Winkler elastic foundation to represent a weak sedimentary layer, such as clay, tuff, or unconsolidated sediments along which laccolith and sill intrusions take place, provides a general geological range for the foundation stiffness parameter $\kappa = 10^4 - 10^9$ N/m^3. Thus, the obtained estimates of the plate thickness $h = 2000$ m and the foundation stiffness parameter $\kappa = 3 \times 10^6$ excellently fit their geophysically reasonable ranges which demonstrates the applicability of the proposed estimation method.

6. Conclusions

In this paper we presented a novel and unique method for estimation of parameters of an elastic plate resting on a Winkler-type foundation solely from the measurements of the vertical displacement of the plate. The method is based on the multiple plate models used in conjunction and allows one to estimate components of the external body force density field, plate thickness, elastic foundation stiffness parameters, as well as horizontal displacements of the plate and stresses. Since neither a single plate model nor a pair of plate models suffices to estimate any of the above mentioned parameters, we employed a family of three plate models - the proposed R3D plate model, the Mindlin plate model, and the thin plate model. The R3D plate model follows the displacement assumptions embedded into the Mindlin plate model, but does not impose zero stress assumptions existing in the thin and Mindlin plate models and does not involve a shear correction factor from the Mindlin plate model. Thus, the three plate models under consideration form a hierarchy of elastic plate models based on assumptions imposed on stresses, with the R3D plate model being the most generalized model and the thin plate model being the most constrained one. This hierarchical relationship among the plate models serves as a source of prior information in the estimation method. The main advantage and important practical benefit of the proposed method is that only data on vertical displacement are needed to estimate the external body force density field acting on an elastic plate, plate thickness, and foundation stiffness parameters. In addition, as a byproduct of this estimation technique, we also obtain estimates of the stresses and horizontal displacements of the plates. The method has the wide range of applications since estimation of external forces and parameters of plate models are of great practical interest in all fields of science and engineering where elastic plates are employed. The applicability of the proposed estimation method is illustrated by a numerical example motivated by geoscience applications dealing with modeling and analysis of laccolith formation.

Acknowledgments. The authors are grateful to Dr. Daniel O'Hara for his assistance with the Henry Mountains data. L. Karlstrom acknowledges support from the National Science Foundation grant EAR 1848554.

References

[1] S. Boudaa, S. Khalfallah, E. Bilotta; *Static interaction analysis between beam and layered soil using a two-parameter elastic foundation*, Int. J. Adv. Struct. Eng. 11 (2019), 21-30. DOI: 10.1007/s40091-019-0213-9.

[2] A. T. Daloglu, C. V. Girija Vallabhan; *Values of k for slab on Winkler foundation*, J. Geotech. Geoenviron. Eng. Vol. 126, No. 5 (2000), 463-471. DOI: 10.1061/(ASCE)1090-0241(2000)126:5(463).

[3] Y. Deng, Z. Zhang, W. Fan, M. Pérez-Gussinyé; *Multitaper spectral method to estimate the elastic thicknessof South China: Implications for intracontinental deformation*, Geosci. Front. 5 (2014), 193-203. DOI: 10.1016/j.gsf.2013.05.002.

[4] G. Duvaut, J. L. Lions; *Inequalities in mechanics and physics*, Springer-Verlag, New York, 1976.

[5] O. Galland, J. Scheibert; *Analytical model of surface uplift above axisymmetric flat-lying magma intrusions: Implications for sill emplacement and geodesy*, J. Volcanol. Geoth. Res. 253 (2013), 114-130. DOI: 10.1016/j.jvolgeores.2012.12.006

[6] M. Gurtin; *An introduction to continuum mechanics*, Academic Press, New York, 2003.

[7] L. Hormander; *Linear partial differential operators*, Springer-Verlag, New York, 1976.

[8] C. B. Hunt, P. Averitt, R. L. Miller; *Geology and geography of the Henry Mountains region, Utah: a survey and restudy of one of the classic areas in geology*, USGS Professional Paper, Vol. 228 (1953).

[9] S. C. Hunter; *Mechanics of continuous media, 2nd ed.*, Ellis Horwood Limited, New York, 1983.

[10] M. D. Jackson, D. D. Pollard; *The laccolith-stock controversy: new results from the southern Henry Mountains*, Utah Geol. Soc. Am. Bull. 100 (1988), 117-139.

[11] T. S. Jang, H. G. Sung, S. L. Han, S. H. Kwon; *Inverse determination of the loading source of the infinite beam on elastic foundation*, J. Mech. Sci. Technol. 22 (2008), 2350-2356. DOI: 10.1007/s12206-008-0822-x.

[12] A. D. Kerr, D. D. Pollard; *Towards more realistic formulations for the analysis of laccoliths*, J. Struct. Geol. Vol. 20, No. 12 (1998), 1783-1793.

[13] J. Lagnese, J. L. Lions; *Modelling analysis and control of thin plates*, Spring-Verlag, New York, 1989.

[14] C. Lanczos; *The variational principles of mechanics, Fourth Edition*, Dover, New York, 1986.

[15] L. D. Landau, E. M. Lifschitz; *Mechanics, Third Edition*, Elsevier, San Francisco, 2005.

[16] S. K. Lee; *Identification of impact force in thick plates based on the elastodynamics and time-frequency method (I) -Theoretical approach for identification the impact force based on elastodynamics*, J. Mech. Sci. Technol. 22 (2008), 1349-1358. DOI: 10.1007/s12206-008-0319-7.

[17] D. G. Luenberger; *Optimization by vector space methods*, Wiley, New York, 1969.

[18] V. G. Maz'ja; *Sobolev spaces*, Springer-Verlag, New York, 1985.

[19] L. Meirovitch. *Analytical methods in vibrations*, McMillan, New York, 1967.

[20] J. E. Michaels, Y.-H. Pao; *The inverse source problem for an oblique force on an elastic plate*, J. Acoust. Soc. Am. 77 No. 6 (1985), 2005-2011. DOI: 10.1121/1.391772.

[21] R. D. Mindlin; *Influence of rotatory inertia and shear on flexural motion of isotropic, elastic plates*, J. Applied Mechanics, Vol. 18 (1951), 31-38.

[22] K. E. Murray, P. W. Reiners, S. N. Thomson; *Rapid Pliocene–Pleistocene erosion of the central Colorado Plateau documented by apatite thermochronology from the Henry Mountains*, Geology 44 No. 6 (2016), 483–486. DOI: 10.1130/G37733.1.

[23] D. O'Hara, L. Karlstrom, J. J. Roering; *Distributed landscape response to localized uplift and the fragility of steady states*, EPSL, 506 (2019), 243-254. DOI: 10.1016/j.epsl.2018.11.006

[24] D. O'Hara, N. Klema, L. Karlstrom; *Development of magmatic topography through repeated stochastic intrusions*, J. Volcanol. Geotherm. Res., 419 (2021), 107371. DOI: 10.1016/j.jvolgeores.2021.107371.

[25] C.-Z. Qu, P. Shao; *An improved method for foundation modulus in highway engineering*, EJGE, Vol 14. (2009), Bund. H: 1-12.

[26] M. Schultz; *Spline analysis*, Prentice-Hall, Englewood Cliffs, N.J., 1973.

[27] O. Steinbach; *Numerical Approximation Methods for Elliptic Boundary Value Problems: Finite and Boundary Elements*, Springer, New York, 2008.

[28] W. T. Strughan; *Analysis of plates on elastic foundations*, Ph.D. Thesis, Texas Tech University, 1990.

[29] A. Tarantola; *Inverse Problem Theory*, Elsevier, New York, 1987.

[30] R. Temam; *Infinite-dimensional dynamical systems in mechanics and physics. Applied mathematical sciences, second ed.*, Vol.68, Springer, New York, 1997.

[31] K. Terzaghi; *Evaluation of coefficients of subgrade reaction*, Ge´otechnique, London, 5 (1955), 297-326.

[32] M. Tesauro, P. Audet, M. Kaban, R. Bürgmann, S. Cloetingh; *The effective elastic thickness of the continental lithosphere: Comparison between rheological and inverse approaches*, Geochem. Geophys. Geosyst., 13 (2012), Q09001. DOI:10.1029/2012GC004162.

[33] H.-T. Thai, T. P. Vo; *A new sinusoidal shear deformation theory for bending, buckling, and vibration of functionally graded plates*, Appl. Math. Model. 37 (2003), 3269-3281.

[34] S. Timoshenko, S. Woinowsky-Kriefer; *Theory of Plates and Shells*, McGraw-Hill, New York, 1959.

[35] G. Wahba; *Spline Models for Observational Data*, SIAM Philadelphia, 1990.

[36] A. Worku; *Winkler's single-parameter subgrade model from the perspective of an improved approach of continuum-based subgrade modeling*, Zede Journal, Vol. 26 (2009), 11-22.

[37] E. Wu, T.-D. Tsai, C.-S. Yen; *Two Methods for Determining Impact-force History on Elastic Plates*, Exp. Mech. 35 (1995), 11-18. DOI: 10.1007/BF02325828.

[38] C.-H. Yen, E. Wu. *On the Inverse Problem of Rectangular Plates Subjected to Elastic Impact, Part I: Method Development and Numerical Verification*, J. Appl. Mech. Vol. 62, No. 3 (1995), 692-698. DOI: 10.1115/1.2896002.

[39] D. Younesian, A. Hosseinkhani, H. Askari, E. Esmailzadeh; *Elastic and Viscoelastic Foundations: a Review on Linear and Nonlinear Vibration Modeling and Application*, Nonlinear Dyn. 97 (2019), 853-895. DOI: 10.1007/s11071-019-04977-9.

[40] H. Zenzri, L. M. Keer; *Mechanical Analyses of the Emplacement of Laccoliths and Lopolith*, J. Geophys. Res. Solid Earth, Vol. 106, No. B7 (2001), 13781-13792. DOI: 10.1029/2001JB000319.

Luther W. White
Oregon Applied Mathematics Institute, 2130 Ridgeway Dr., Eugene, OR 97401, USA
Email address: oregami.lwhite@gmail.com

Tetyana Malysheva
Department of Mathematics & Statistics, Resch School of Engineering, University of Wisconsin-Green Bay, 2420 Nicolet Drive, Green Bay, WI 54311, USA
Email address: malyshet@uwgb.edu

Leif Karlstrom
Department of Earth Sciences, 1272 University of Oregon, Eugene, OR 97403, USA
Email address: leif@uoregon.edu